Involvement of caveolin-1 in the Jak–Stat signaling pathway and infectious spleen and kidney necrosis virus infection in mandarin fish (*Siniperca chuatsi*)

Chang-Jun Guo [a,b,1], Xiao-Bo Yang [b,1], Yan-Yan Wu [b], Li-Shi Yang [b], Shu Mi [b], Zhao-Yu Liu [b], Kun-Tong Jia [b], Yu-Xin Huang [b], Shao-Ping Weng [b], Xiao-Qiang Yu [c,**], Jian-Guo He [a,b,*]

[a] *MOE Key Laboratory of Aquatic Product Safety/State Key Laboratory for Biocontrol, School of Marine Sciences, Sun Yat-sen University, 135 Xingang Road West, Guangzhou 510275, PR China*
[b] *State Key Laboratory for Biocontrol, School of Life Sciences, Sun Yat-sen University, 135 Xingang Road West, Guangzhou 510275, PR China*
[c] *Division of Cell Biology and Biophysics, School of Biological Sciences, University of Missouri-Kansas City, Kansas City, MO 64110, USA*

ARTICLE INFO

ABSTRACT

Caveolae, the major source of caveolin-1 protein, are specialized invaginated microdomains of the plasma membrane that act as organizing centers for signaling molecules in the immune system. In the present study, we report the cloning and characterization of caveolin-1 (mCav-1) from mandarin fish (*Siniperca chuatsi*) and study on the roles of mCav-1 in the fish Jak–Stat signaling pathway and in virus infection. The cDNA sequence of mCav-1 was 707 bp in size, encoding a protein of 181 amino acids, which was different from the mammalian protein (178 amino acids). The deduced amino acid sequence of mCav-1 shared similar architecture with vertebrate caveolin-1 proteins, but mCav-1 lacked a phosphorylation site (y14). The major subcellular location of mCav-1 was in the caveolae, where the protein appeared to have major functions. Real-time PCR revealed that the expression of the mandarin fish *Mx*, *IRF-1*, *SOCS1*, and *SOCS3* genes involved in the poly(I:C)-induced Jak–Stat signaling pathway was impaired by the mCav-1 scaffolding domain peptide (mSDP). In mandarin fish fry (MFF-1) cells, the protein levels of mCav-1 were markedly up-regulated at 12 and 24 h post-infection with ISKNV (infectious spleen and kidney necrosis virus). In addition, ISKNV entry into MFF-1 cells was significantly inhibited by mSDP, and the inhibition was dose-dependent. Thus, ISKNV infection was apparently associated with mCav-1 protein and may utilize the caveolae-related endocytosis pathway. The findings reported here further our understanding of the function of caveolin-1 in the complex signal transduction network in fish immune systems and in the cellular entry mechanism of iridoviruses.

© 2011 Elsevier Ltd. All rights reserved.

1. Introduction

Caveolae are specialized flask-shaped invaginations 50–100 nm in diameter within the plasma membrane (Palade, 1953). They are found in most mammalian cells, but are particularly abundant in terminally differentiated cells, such as adipocytes, endothelial cells, smooth muscle cells, and fibroblasts (Rothberg et al., 1992). Caveolae are highly enriched in cholesterol and glycosphingolipids and are characterized by the presence of caveolin proteins (Thomas and Smart, 2008).

The caveolins are a family of 21–24 kDa integral membrane proteins that bind cholesterol and fatty acids and that also maintain the structure of caveolae (Ikonen and Parton, 2000). Three members of the caveolin family have been identified to date: caveolin-1 (Cav-1, previously named VIP-21), caveolin-2 (Cav-2), and caveolin-3 (Cav-3, previously named M-caveolin) (Williams and Lisanti, 2004; Way and Parton, 1996). Caveolin-1 was first identified as a principal protein component of caveolae membranes (Kurzchalia et al., 1992). Subsequently, caveolin-1 was found highly expressed in cells with abundant caveolae and caveolin-1 expression was also found necessary or sufficient to generate caveolae membranes (Kim et al., 2006). Caveolin-1 directly binds to cholesterol, employing the "cholesterol recognition amino acid consensus" sequence composed of residues 95–101 in the caveolin scaffolding domain (CSD). The cholesterol-binding capacity of caveolin-1 plays a key role in maintaining a stable balance of intracellular cholesterol, allowing caveolin-1 to act as a transporter that directs cholesterol efflux, selective uptake, and the delivery of newly synthesized cholesterol to the plasma membrane (Fielding, 2006). The membrane binding

and lipid raft interactions of synthetic peptides derived from the CSD of the caveolin-1 protein (caveolin-1 scaffolding domain peptide, SDP) have been investigated (Horton et al., 2006; Benferhat et al., 2008).

Caveolin-1 clearly plays important roles in cholesterol transport, endocytosis, and signal transduction (Frank et al., 2008). It is thought to function as a scaffolding protein that organizes and concentrates cholesterol, glycosphingolipids, and caveolae-associated signaling molecules, such as endothelial nitric oxide synthase, H-ras, Src-like kinase, G proteins, Janus kinase (Jak), and signal transducer and activator of transcription (Stat) proteins, among others (Couet et al., 1997; Ju et al., 1997; Harris et al., 2002; Schutzer et al., 2005; Baran et al., 2007; Elsasser et al., 2007; Rath et al., 2009). Caveolae are known to act as organizing centers for immune-related signal transduction pathways, such as the Jak–Stat signaling pathway or the NFκB–IκB signaling pathway, etc. (Harris et al., 2002; Garrean et al., 2006). In mammals, the Jak–Stat signaling pathway functions in host defense against viral and bacterial infections (Lad et al., 2005; Haller and Weber, 2009). The Jak–Stat signal transduction pathway is activated by a large number of cytokines and growth factors, including interferon (IFN)-α/β, IFN-γ, interleukin-2 (IL-2), IL-4, IL-5, IL-6, IL-10, and growth hormone (GH), among others (Imada and Leonard, 2000; Levy and Darnell, 2002; Gao, 2005; Chelbi-Alix and Wietzerbin, 2007; Sarasin-Filipowicz et al., 2009). In mammalian cells, caveolin-1 protein has been reported to inhibit the Jak–Stat signaling pathway through direct interaction with Stat3 protein (Shah et al., 2002).

The mandarin fish, *Siniperca chuatsi* (Basilewsky), is widely cultured and has a relatively high market value in China (Liu et al., 1998, 2000). However, outbreaks of disease caused by pathogenic parasites, bacteria, and viruses, especially the infectious spleen and kidney necrosis virus (ISKNV), now greatly threaten the aquaculture industry (He et al., 2000; Zhang et al., 2003; Sun and Nie, 2004). For this reason, research is being conducted to understand the immune system of the mandarin fish. The primary structure and functional roles of caveolin-1 protein have been described in other vertebrates, such as humans, mice, sheep, rabbits, and frogs, etc. (Glenney and Soppet, 1992; Sargiacomo et al., 1993; Tang et al., 1994; Lavialle et al., 2000; Chen et al., 2001). However, the biological roles of caveolin-1 with respect to immune responses in fish are still not well understood.

In the current study, the molecular cloning, tissue-specific expression, and subcellular distribution of mandarin fish caveolin-1 were reported. A functional role for this protein in the poly(I:C)-induced Jak–Stat signal transduction pathway and in virus infection was also postulated.

2. Materials and methods

2.1. Experimental animal, cell and virus

Healthy mandarin fish (weight ~250 g) were obtained from a fish farm in Nan-Hai (Guangdong Province, China) and maintained for at least 2 weeks in aquaria at 28 °C. Freshly dissected tissues, including brain, fat tissue, heart, hemocytes, gills, intestines, liver, muscle, kidney, and spleen, were washed thoroughly with phosphate buffered saline (PBS) and immediately homogenized with thiourea lysis buffer (7 M urea, 2 M thiourea, 4% CHAPS) containing protease inhibitor cocktail set III (Calbiochem, USA). Protein concentrations were quantified using the Bradford reagent (Bio-Rad, USA) and 100 μg of protein was analyzed by Western blotting.

Mandarin fish fry (MFF-1) cells were cultured in Dulbecco's modified Engle's medium (DMEM) supplemented with 10% fetal bovine serum (FBS) at 27 °C under a humidified atmosphere containing 5% CO_2 (Dong et al., 2008). The ISKNV used in this study was originally isolated from diseased mandarin fish and maintained by our laboratory. For infection, MFF-1 cells were cultured in 25 cm^2 flasks at 5×10^6 cells overnight before further treatment. Each flask was inoculated with virus suspension (MOI = 10) and cells were harvested at various times (1, 2, 4, 8, 12, and 24 h), while the uninfected flask served as a negative control.

2.2. Molecular cloning and sequence analysis of mCav-1

Total RNA was extracted from MFF-1 cells using Trizol reagent (Invitrogen, USA) and reverse transcribed to cDNA as previously described (Guo et al., 2009). A cDNA fragment of mCav-1 was obtained by PCR amplification with degenerate primers mCav-1-F and mCav-1-R (Table 1), which were derived from conserved regions of known caveolin-1 sequences. The PCR fragment was subcloned into the pGEM-T Easy vector (Promega, USA) and selected clones were sequenced. Based on the obtained partial sequence of mCav-1, gene-specific primers were designed (Table 1) and 3′/5′ RACE was performed using a GeneRacer Kit (Invitrogen, USA). The PCR products were gel-purified and subcloned into the pGEM-T Easy vector for DNA sequencing.

The cDNA sequence and deduced amino acid sequence of mCav-1 were analyzed using the BLAST program from NCBI and the Simple Modular Architecture Research Tool (SMART) program. Sequence alignments were performed using the ClustalX v1.83 program and edited with the GeneDoc v2.6 software (Thompson et al., 1997).

2.3. Prokaryotic expression of mCav-1 and preparation of its polyclonal antibody

Based on the complete open reading frame sequence of mCav-1, a pair of primers (MBP-mCav-1-F and -R, Table 1) was designed. The DNA fragment was amplified by PCR, digested with EcoR I and Xba I, and then inserted into the expression vector pMAL-C2X (New England Biolabs, UK), which expresses a maltose binding protein (MBP). The resultant plasmid, designated as pMAL-mCav-1, was transformed into the competent *E. coli BL21* strain. MBP and the mCav-1 fusion protein (named MBP-mCav-1) were expressed after induction with 0.1 mM IPTG for 4 h at 37 °C, and the supernatants of sonicated bacterial cells were analyzed by SDS-PAGE.

Table 1
Primers used for cloning mCav-1.

Primer name	Sequence (5′–3′)	Use
mCav-1-F	AAGRTDGAYTTTGARGAYGTGATCGC	mCav-1 partial
mCav-1-R	CASTGGATCTCGATYAGGTARCTC	mCav-1 partial
3′-mCav-1-F1	TCTTCTTCGCCATCCTGTCC	mCav-1 3′ RACE
3′-mCav-1-F2	CGTGCGTCAAGAGCTACCTAATCGAGATC	mCav-1 3′ RACE
5′-mCav-1-R1	TCAGCAGCCGGTAGCACC	mCav-1 5′ RACE
5′-mCav-1-R2	CCCTGCAGGCTCGGCGATCAC	mCav-1 5′ RACE
MBP-mCav-1-F	CGGGAATTCACAGGAGGACTGAAGGACGATG	Cloned into expression vector
MBP-mCav-1-R	GCTCTAGACTACACCTCCTTGGTCGTGCG	Cloned into expression vector

R = A/G; Y = C/T; S = C/G; D = A/G/T.

In addition, as a control, the pMAL-C2X vector was also expressed and the MBP protein was purified. The MBP-mCav-1 protein was purified using an amylase affinity resin column (New England Bio-labs, UK) and separated by SDS-PAGE gels, followed by collection of the single bands of MBP-mCav-1 protein (~500 μg) from the gels. The MBP-mCav-1 protein bands were ground and mixed with 1 ml of complete Freund's adjuvant (Sigma, USA) and the mixture was subcutaneously injected into New Zealand white rabbits (Laboratory Animal Research Centre, Sun Yat-sen University, China) (designated Day 1). Booster immunizations of purified MBP-mCav-1 fusion protein in 1 ml of Freund's incomplete adjuvant (Sigma, USA) were given to each rabbit on days 14, 21, and 28. Four days after the last injection, rabbits were exsanguinated and antisera were collected. After titer determination by Western blot, the antiserum was stored at −80 °C.

2.4. Isolation of caveolae-enriched fractions from MFF-1 cells

MFF-1 cells were treated with 2.0 mM methyl-β-cyclodextrin (MβCD, Sigma, USA), 50 μg/ml filipin III (Sigma, USA), and 50 μg/ml nystatin (Sigma, USA) for 60 min at 27 °C. Preparation of caveolae-enriched membrane fractions was performed as previously described (Smart et al., 1995; Song et al., 1996). Briefly, cells were washed twice with ice-cold PBS and scraped into 1 ml of 25 mM MES hydrate buffer (pH 6.5), containing 25 mM MES, 0.15 M NaCl, 5 mM EDTA, and 1% Triton X-100 (MBS) with protease inhibitors (10 μg/ml aprotinin, 10 μg/ml leupeptin, 1 mM sodium orthovanadate, 10 mM NaF, 1 mM Pefabloc) and kept on ice for 30 min. The suspension was subjected to 10–15 strokes in a Dounce homogenizer and centrifuged for 10 min at $2000 \times g$ at 4 °C to remove nuclei. Clarified postnuclear supernatants were combined with 90% (w/v) sucrose prepared in MBS, transferred to the bottom of a Beckman 12.5-ml ultracentrifuge tube, and overlaid gently with 6 ml of 35% and 3 ml of 5% sucrose, respectively. The resulting 5–40% discontinuous sucrose gradients were centrifuged for 18–20 h at $39,000 \times g$ in a SW41 Beckman rotor at 4 °C in order to allow the separation of caveolae.

2.5. Western blot analysis

Protein samples were separated by SDS-PAGE on either 12 or 15% gels and then transferred to nitrocellulose membranes (Whatman, USA). After blocking overnight at 4 °C in PBST (0.05% Tween-20 in PBS) containing 5% (w/v) milk power, the membranes were incubated with primary antibodies (mCav-1 antisera and anti-MBP antiserum diluted 1:2000 in blocking buffer) for 2 h at room temperature and then washed three times in PBST. After 60 min incubation with 1:5000 diluted AP-conjugated goat anti-mouse or HRP-conjugated goat anti-mouse antibodies, the membranes were rinsed three times with PBST. Immunosignals were detected by BCIP/NBT, or by enhanced chemiluminescence reagent (Pierce, USA) followed by exposure of polyvinylidene difluoride membranes to Hyperfilm (Amersham Biosciences, Piscataway, NJ, USA).

2.6. Indirect immunofluorescence assay (IFA)

Cells were attached to glass slides coated with L-lysine in a humidified chamber. Cell monolayers were rinsed with PBS and fixed with chilled 100% methanol at −20 °C for 5 min, and permeabilized with 0.05% Triton X-100 in PBS for 5 min. After 1 h incubation in a blocking buffer (PBS, 5% goat serum, and 1% BSA), the cells were reacted with antisera against mCav-1 (1:200 dilution with a blocking buffer) at 37 °C for 2 h. After washing five times with PBS for 5 min each wash, the cells were incubated with Alexa Fluor®-555 conjugated anti-mouse IgG (Invitrogen; 1:300 dilution in blocking buffer) at 37 °C for 45–60 min. As a control, fixed cells were incubated with mouse pre-immune serum instead of anti-mCav-1 antiserum. After staining with Hoechst 33342 (Invitrogen, USA), the glass coverslips were removed from the wells and observed with a laser scanning confocal microscope (Leica TCS-SP2, Germany).

2.7. mCav-1 scaffolding domain peptide (mSDP) and cell viability

The mCav-1 scaffolding domain peptide (mSDP), corresponding to the full-length sequence (amino acids 85–104; DGVWKAS-FTTFTVTKYWCYR), was synthesized as a fusion peptide to the C terminus of the Antennapedia internalization sequence (RQIKIWFQNRRMKWKK) by standard fluorenylmethoxycarbonyl chemistry and analyzed by mass spectrometry to confirm purity by the Sangon Biological Engineering Technology & Service Co. Ltd (Shanghai, China). Before each experiment, desiccated peptides were weighed, dissolved in DMSO to 100 mM, and diluted to 1 mM with distilled water.

The cytotoxicity of mSDP was evaluated using the Cell Counting Kit (CCK-8, Beyotime, Jiangshu, China). In brief, 5×10^3 MFF-1 cells per well were plated in a 96-well plate and incubated at 27 °C for 24 h, at which point the medium was replaced with fresh medium. Cells were then treated with the indicated concentrations of mSDP incubated at 27 °C for an additional 6 h. CCK-8 solution (10 μl) was added to each well, and cells were incubated for 1 h. The absorbance of each well was measured at 450 and 570 nm with an ELISA reader.

2.8. Effects of mSDP on the poly(I:C)-induced Jak–Stat signaling pathway

MFF-1 cells were pretreated with mSDP (10 μM) for 30 min, and cells were incubated in medium with 0.1% DMSO as a control. Cell culture supernatants were replaced with DMEM medium supplemented with 10 μg/ml concentration of polyinosinic:polycytidylic acid [poly(I:C), Sigma, USA], and incubated in the presence of 10 μM mSDP or 0.1% DMSO. Cells were harvested by centrifugation at various times after treatment (2, 4, 6, 8, 12, 16, 24, 48, 72, 96, and 120 h). Total RNA was extracted and reverse transcribed to cDNA. The expression of the Mx, IRF-1, SOCS1, SOCS3 genes were investigated by quantitative RT-PCR on a LightCycler (Roche Diagnostics, Switzerland) as previously described (Guo et al., 2009). β-Actin, a housekeeping gene, was used as a control. The expression levels of each transcript were normalized to β-actin expression. The real-time quantitative PCR data of target genes were analyzed using the Q-gene statistics add-in followed by unpaired sample t-test (Muller et al., 2002). Statistical significance was accepted at $p < 0.01$. All data were expressed as means ± standard deviations (SD).

2.9. Effects of mSDP on ISKNV infection

Cells were plated in 48-well/6-well plates and grown to approximately 80% confluence at 27 °C. Cells were either untreated or pretreated for 1 h with various concentrations of mSDP. After treatment, the cells were infected with ISKNV for 4 h at 27 °C, in the presence of mSDP. Noninternalized viruses were removed by removing virus inocula and washing the cells with citrate buffer (40 mM sodium citrate, 10 mM KCl, 135 mM NaCl, pH 3.0) for 1 min at room temperature (Kizhatil and Albritton, 1997). Western blotting and immunofluorescence analysis for ISKNV membrane protein ORF101L expression were carried out at 72 h post-infection.

3. Results

3.1. Molecular characteristics of the full-length mCav-1

The full-length cDNA sequence of mCav-1 cDNA was obtained by amplification with degenerate primers and RACE technology.

A

```
1    5' GATTGGACACTGACATGGACTGAAGGAGTAGAAAAAACTTGGGGAGAGC ATG ACA GGA GGA CTG
                                                          M   T   G   G   L

65   AAG GAC GAT GAA ACA GAA GAG AAG TTT CTG CAT TCG CCG TTC ATC CGA AAA CAA
     L   K   D   D   E   T   E   E   K   F   L   H   S   P   I   R   K   Q

119  GGG AAC ATA TAC AAA CCT AAC AAC AAA GAC ATG GAC AAC GAC AGT CTG AAC GAG
     G   N   I   Y   K   P   N   N   K   D   M   D   N   D   S   L   N   E

173  AAA ACG ATG GAG GAT GTC CAC ACC AAA GAG ATC GAC TTG GTC AAC CGT GAC CCA
     K   T   M   E   D   V   H   T   K   E   I   D   L   V   N   R   D   P

227  AAG CGC ATA AAC GAT GAC GTT GTC AAG GTA GAG TTT GAG GAT GTG ATC GCC GAG
     K   R   I   N   D   D   V   V   K   V   E   F   E   D   V   I   A   E

281  CCT GCA GGG AAT CAC AGC TTC GAC GGT GTG TGG AAA GCC AGC TTC ACC ACC TTC
     P   A   G   T   Y   S   F   D   G   V   W   K   A   S   F   T   T   F

335  ACC GTC ACC AAG TAC TGG TAC CGG CTG CTG ACG GCG CTG GTC GGC ATC CCC
     T   V   T   K   Y   W   C   Y   R   L   L   T   A   L   V   G   I   P

389  CTG GCA CTG ATC TGG GGA ATC TTC TTC GCC ATC CTG TCC TTC ATA CAC ATC TGG
     L   A   L   I   W   G   I   F   F   A   I   L   S   F   I   H   I   W

443  GCT GTG GTG CCG TGC GTC AAG AGC TAC CTA ATC GAG ATC CAC TGC GTC AGT CGT
     A   V   V   P   C   V   K   S   Y   L   I   E   I   H   C   V   S   R

497  GTC TAC TCC ATC TGC GTG CAC ACC TTC TGC GAC CCG TTG TTT GAA GCC ATG GGC
     V   Y   S   I   C   V   H   T   F   C   D   P   L   F   E   A   M   G

551  AAG TGC TTC AGC AGC GTC CGA ATC CGC ACG ACC AAG GAG GTG TAG ATCCGCAAAGAG
     K   C   F   S   S   V   R   I   R   T   T   K   E   V

608  GAGGAGGAGTATTAACGGAAAGAGGGGAGGGAGGATGGGAGGGCTAGAGCCACACAGATGGAGGGAAAAGC
679  CAGAACAAAAAAAAAAAAAAAAAAAAAAAAA 3'
```

B
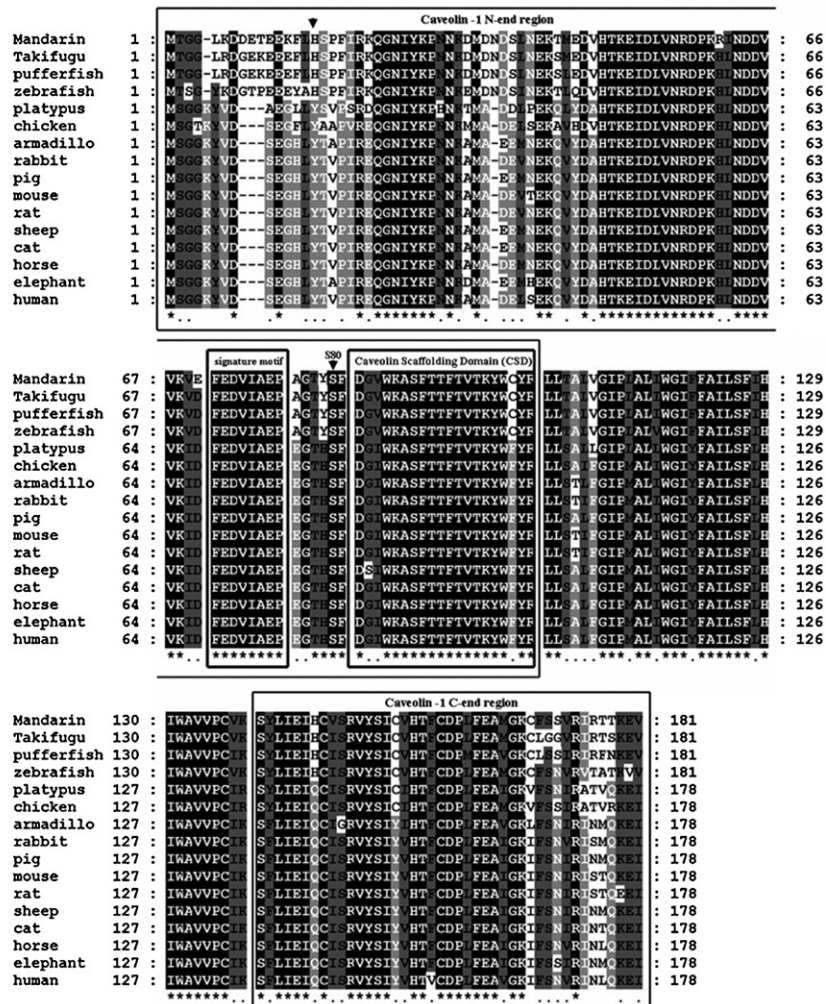
Fig. 1. (A) Nucleotide and deduced amino acid sequences of mandarin fish caveolin-1 (accession no. FJ695596). The start and stop codon features are highlighted. The sequence of caveolin scaffolding domain (CSD) is boxed. (B) Multiple alignment of mCAV-1 with the currently known caveolin-1 proteins from mammals, birds, amphibians, and fish. The dashes in the amino acid sequences indicate gaps introduced to maximize alignment. Identical (*) and similar (.) resides identified by the ClustalX v1.83 program are indicated. The N-end region, signature motif (FEDVIAEP), caveolin scaffolding domain, and C-end region are boxed.

BLAST homology analysis showed close matches of mCav-1 with caveolin-1 from other vertebrates. The complete sequence of mCav-1 cDNA was 707 bp and contained a 5′-UTR of 49 bp, followed by an open reading frame (ORF) of 546 bp encoding a predicted protein of 181 amino acid residues and a 3′-UTR of 112 bp, including 23 nucleotides of the polyadenylation tail. The full-length sequence of mCav-1 was deposited in GenBank under accession no. FJ695596, and the deduced amino acid sequence was determined (Fig. 1A). Two potential translation start sites were observed within the N terminus of the mCav-1 gene, which indicated mCav-1 might occur as two isoforms (α- and β-isoforms). The SMART program results showed that the deduced amino acid sequences of the mCav-1 shared similar architecture of vertebrate caveolin-1 proteins, but mCav-1 lacked a phosphorylation site (y14). Multiple amino acid alignments of mCav-1 with other known vertebrate caveolin-1 molecules revealed a significant homology with the other known caveolin-1 sequences present in the database. Bioinformation analysis showed that the deduced amino acid sequences of the mCav-1 share a similar architecture with vertebrate caveolin-1 proteins, including a N-end region, a signature motif (FEDVIAEP), a caveolin scaffolding domain, and a C-end region (Fig. 1B). The mCav-1 had highest amino acid identity (above 90%) and similarity (above 95%) with caveolin-1 proteins from zebrafish (*Danio rerio*), pufferfish (*Tetraodon nigroviridis*), and fugu (*Takifugu rubripes*) compared with other vertebrate caveolin-1 proteins.

3.2. Immunofluorescence and Western blot analysis of mCav-1 cellular distribution

The cellular distribution of mCav-1 protein in MFF-1 cells was determined by immunofluorescence and Western blot analysis (Fig. 2A and B). The anti-mCav-1 antiserum used in our work was generated in New Zealand white rabbits by immunization with purified MBP-mCav-1 fusion protein. Fluorescence microscopy showed mCav-1 (red fluorescence) to be located in the plasma membrane and cytoplasm with dot distribution in MFF-1 cells, whereas mCav-1 was not observed in the nucleus (blue fluorescence) (Fig. 2A). A detergent-free method for preparing cholesterol-enriched fractions from MFF-1 cells was used. Cave-

olae are resistant to nonionic detergents and could be extracted by ultracentrifugation in a sucrose gradient followed by 1% Triton X-100 treatment (Beer et al., 2005). The detergent-resistant membranes (DRMs) that are buoyant on low-density sucrose gradients have unique caveolae enriched with cholesterol, glycolipids, and caveolin proteins. Equal volume fractions of DRM and detergent-soluble membranes (DSMs) were separated by gel electrophoresis and subjected to Western blotting using anti-mCav-1 antiserum. As shown in Fig. 2B, mCav-1 protein was detected in the DRM (Fig. 2B, lanes 4–9) but was absent in the DSM (Fig. 2B, lanes 10–12). These results were consistent with the typical distribution of caveolin-1 in mammalian cells (Parkin et al., 1996). MβCD, fillipin III, or nystatin (which deplete or sequester membrane cholesterol) is employed to disrupt the caveolae structure (Foster et al., 2003; Lee et al., 2008, 2009). As shown in Fig. 2C, the distribution of mCav-1 was altered and enriched in the DSM fractions (Fig. 2C, lanes 10–12) when cells were treated with MβCD, filipin III, or nystatin, whereas in cells not treated with drugs, mCav-1 was found primarily in the DRM (Fig. 2C, lanes 4–9). In addition, the electron micrographs show typical membrane invaginations found at the plasma membrane of MFF-1 cells (Fig. 2D, arrows). These results suggested that the major subcellular location for mCav-1 was in caveolae.

3.3. Immunoblotting analysis of the tissue-specific distributions of mCav-1

The most thorough analysis of tissue-specific expression of caveolin-1 has been conducted in mammals and amphibians (Scherer et al., 1996; Tang et al., 1996; Razani et al., 2002). However, the tissue expression pattern of caveolin-1 has not yet been rigorously studied in fish. To establish the tissue-specific distribution of caveolin-1 protein in mandarin fish, we prepared extracts from a number of different tissues and used immunoblotting assays to compare the mCav-1 expression levels. Equal weights (~100 μg) of each tissue were separated by gel electrophoresis and immunoblotted with anti-mCav-1 antiserum. As shown in Fig. 3, mCav-1 protein had two isoforms (α- or β-isoform) that were detected in most tissues. This was different from expression of endogenous mCav-1 in MFF-1 cells, where only the α-isoform was
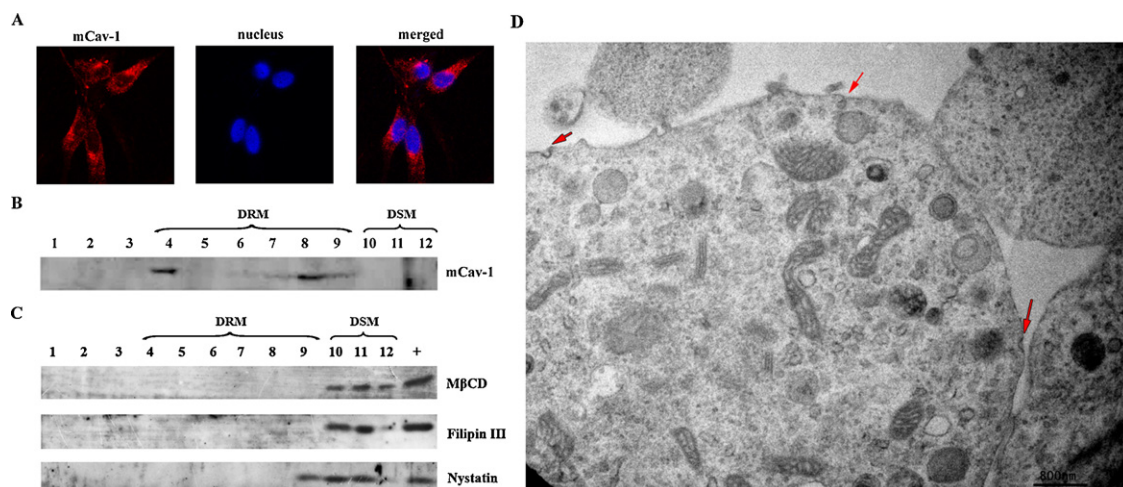
Fig. 2. Subcellular distribution of mCav-1 protein in MFF-1 cells. (A) Immunofluorescence analysis of mCav-1 protein in MFF-1 cells. The red fluorescence was immunostained by anti-mCav-1 antiserum, and the blue fluorescence was immunostained by Hoechst 33342. Magnification: ×400. (B) Western blot analysis of mCav-1 protein. Cholesterol-rich fractions were isolated by 1% Triton X-100 treatment and ultracentrifugation in a sucrose gradient. After centrifugation, the total proteins in each fraction were separated by gel electrophoresis and immunoblotted with anti-mCav-1 antiserum. Lanes 1–12 are sucrose gradient fractions (top to bottom); lanes 4–9 are the DRM (detergent-resistant membrane) fractions (caveolae fragments); lanes 10–12 are the DSM (detergent-soluble membrane) fractions (cytoplasm fragments). (C) MβCD, filipin III, and nystatin altered the distribution of mCav-1 protein. Cells either were not treated or were incubated in the presence of MβCD, filipin III, or nystatin for 60 min before isolation of the cholesterol-rich fractions. Each fraction was immunoblotted with anti-mCav-1 antiserum. Lanes 1–12 are the sucrose gradients fractions (top to bottom); lanes 4–9 are the DRM fractions; lanes 10–12 are the DSM fractions; the last lane is lysate from MFF-1 cells before extraction of cholesterol-rich fractions. (D) Electron microscopy. Caveolae were identified and observed close to the plasma membrane in MFF-1 cells (arrows). Scale bars: 800 nm. (For interpretation of the references to color in this figure legend, the reader is referred to the web version of the article.)
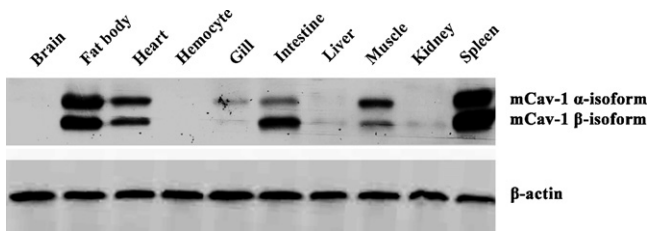
Fig. 3. Western blot analyses of the tissue-specific distribution of caveolin protein in mandarin fish. Protein lysates from the indicated tissues of healthy mandarin fish were prepared and 100 μg was subjected to SDS-PAGE and immunoblot analysis using anti-mCav-1 antiserum. β-Actin was employed an internal control protein.

detected. The α- or β-isoforms were expressed in the fat tissue, heart, gills, intestine, liver, skeletal muscle, kidney, and spleen, but were not detected in the brain or hemocytes. On a tissue weight basis, the levels of the α-isoform were generally higher than the levels of the β-isoform in fat tissue, heart, gills, and skeletal muscle. Consistent with the large numbers of invaginated caveolae in other vertebrate tissues, mCav-1 was prevalent in smooth muscle (e.g., intestine) and adipocytes (e.g., fat tissues). High levels of mCav-1 protein were also expressed in heart tissue, which appeared to contain as much as skeletal muscle. The highest level of mCav-1 was in the spleen, which, interestingly, is not considered to have large numbers of caveolae (Frank et al., 2009). The spleen, however, is an important immune organ of mandarin fish and was also the major target tissue for ISKNV (He et al., 2001), which suggested that mCav-1 might be involved in immune function.

3.4. Poly(I:C)-induced Jak–Stat signaling pathway was impaired by mSDP

To determine whether caveolin-1 protein regulates the Jak–Stat signal transduction pathway of fish immune systems, the effects of the mCav-1 scaffolding domain peptide on the Jak–Stat signaling pathway were measured in MFF-1 cells. A real-time PCR was performed to analyze the expression of *Mx*, *IRF-1*, *SOCS1*, and

SOCS3 genes involved in the poly(I:C)-induced Jak–Stat at different time intervals (Guo et al., 2009). As shown in Fig. 4, the *mMx*, *mIRF-1*, *mSOCS1*, and *mSOCS3* genes were significantly induced by poly(I:C) post-stimulation of MFF-1 cells (Fig. 4, black columns, as positive controls), compared to the untreated controls (0 h). However, when cells were treated with mSDP and poly(I:C), expression of the *mMx*, *mIRF-1*, *mSOCS1*, and *mSOCS3* genes was significantly lower than those in the positive groups (Fig. 4, gray columns, $p < 0.01$). For instance, expression of the *mMx* gene was markedly increased ~350-fold by treatment of the cells with poly(I:C) for 8–12 h, compared to the untreated controls (0 h), while the expression of the *mMx* gene was increased ~180-fold and noticeably decreased by treatment of the cells with poly(I:C) and mSDP ($p < 0.01$). These results revealed that the poly(I:C)-induced Jak–Stat signal transduction pathway was impaired by the mCav-1 scaffolding domain peptide in MFF-1 cells.

3.5. mCav-1 protein levels were up-regulated in MFF-1 cells infectious with ISKNV

To determine whether mCav-1 was involved in host responses to viral infection, the levels of mCav-1 protein were measured after MFF-1 cells were infected with ISKNV. Cells were harvested and lysed at 1, 2, 4, 8, 12, and 24 h after infection with ISKNV (MOI = 10). The same amounts of total protein were separated by gel electrophoresis and immunoblotted with anti-mCav-1 antiserum. Endogenous β-tubulin was included as an internal loading control for the Western blots, using monoclonal antibodies (MAbs) against β-tubulin (Epitomic Inc.). As shown in Fig. 5A, the mCav-1 protein was detected in all samples, and the levels of mCav-1 protein showed no obvious variation at 1–8 h after infection with virus when compared to uninfected (mock) samples. However, the mCav-1 protein levels were clearly up-regulated at 12 h and 24 h after virus infection. The densitometric analysis of mCav-1 expressions showed that the mCav-1 protein was significantly increased at 12 h (~2.8-folds, $p < 0.05$) and 24 h (~4.6-folds, $p < 0.01$) after ISKNV infection (Fig. 5B).
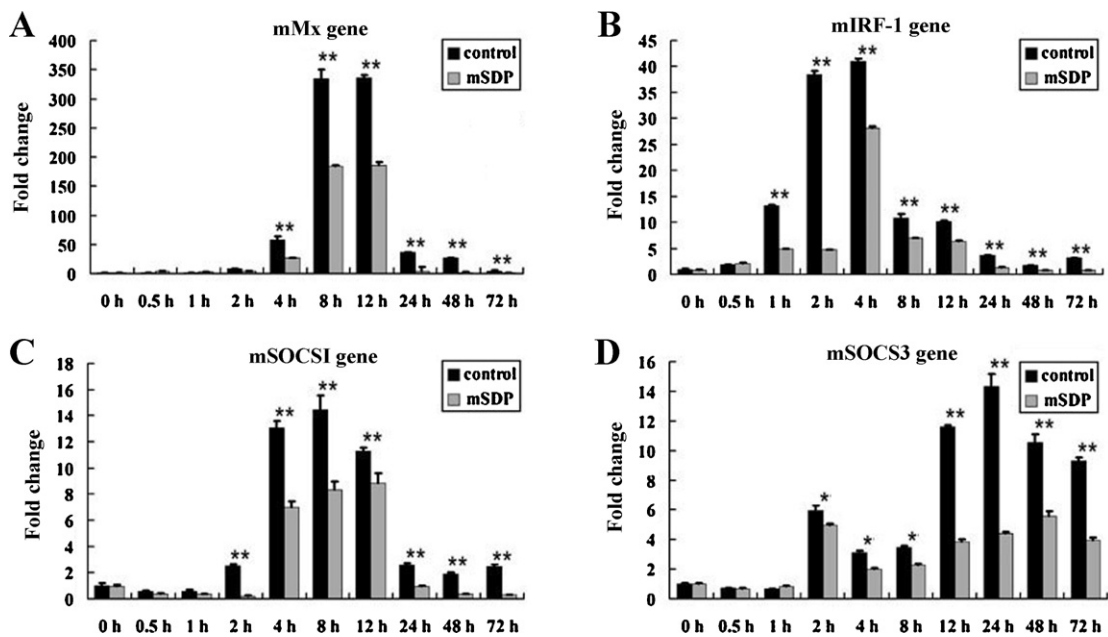
Fig. 4. Time-course expressions of four genes involved in the Jak–Stat signal transduction pathway for different time intervals in MFF-1 cells stimulated by poly(I:C): (A) *mMx*, (B) *mIRF-1*, (C) *mSOCS1*, and (D) *mSOCS3*. After incubation with 10 μM mSDP or 1% DMSO (as a control) for 60 min, cells were treated with 10 μg/ml poly(I:C) stimulation and incubated in the presence of mSDP/DMSO for 2–120 h prior to RNA isolation. The relative expression of each gene was determined by real-time PCR. β-Actin was amplified from the same RNA samples as a control. The basal expression level of each gene (0 h) was arbitrarily set as 1. All data were analyzed by the Q-gene statistics add-in followed by unpaired sample *t*-tests. Error bars represent the means ± SD (*n* = 3). *$p < 0.05$, **$p < 0.01$.
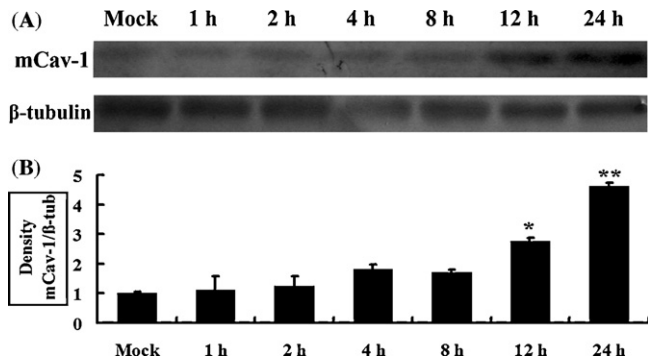
Fig. 5. (A) Western blotting analysis of mCav-1 expression. Cell extracts were harvested at 1, 2, 4, 8, 12, and 24 h after infection with ISKNV (MOI = 10). The same amounts of total protein (80 μg) were immunoblotted with anti-mCav-1 antiserum. β-Tubulin was used as an internal control protein. The uninfected control sample is marked as Mock. (B) Densitometric analysis of mCav-1 expression. The densitometric measurements of mCav-1 proteins are normalized to the β-tubulin protein detected and expressed as a percentage of the average values measured in the mock group. Data are represented as the mean ± SEM. $^*p < 0.05$, $^{**}p < 0.01$.

3.6. ISKNV infection with MFF-1 cells was inhibited by mSDP

In order to determine the mSDP involved in the ISKNV infection, the cytotoxicity of mSDP was evaluated using the CCK-8. The results showed that cell viability was not significant changed when cells were treated with 10 μM mSDP compared to the control cells (Fig. 6A). The entry of ISKNV into MFF-1 cells and its potential association with mCav-1 were examined in cells treated with mSDP and then infected with ISKNV virus. Infections were scored by measuring expression of the ISKNV membrane protein ORF101L using immunofluorescence staining. As shown in Fig. 6A, mSDP concentrations higher than 1 μM significantly inhibited ISKNV entry into cells and the inhibition was dose-dependent. Treatment with 5, 10, 20, and 30 μM mSDP significantly inhibited ISKNV infection by 75, 90, 95, and 98%, respectively, compared to the untreated control (0 μM mSDP). Similar inhibitory effects were also observed by Western blotting. As shown in Fig. 6B, the ORF101L protein levels were significantly reduced when cells were treated with 5, 10, and 25 μM mSDP, compared to the untreated control (0 μM). The expression of ORF101L was almost undetectable when cells were treated with 25 μM mSDP. These results suggested that ISKNV infection was associated with mCav-1 protein, and that viral entry may involve the caveolae-related endocytosis pathway.

4. Discussion

In the present study, we reported the cloning and characterization of mandarin fish caveolin-1 (mCav-1), and studied the potential roles of mCav-1 in the fish Jak–Stat signaling pathway and in ISKNV infection.

The cDNA sequence of mCav-1 was 707 bp in size, encoding a protein of 181 amino acids, which is different from that of mammals (178 amino acids). Bioinformatics analysis showed that the deduced amino acid sequences of mCav-1 shared a similar architecture with vertebrate caveolin-1 proteins and had a high identity score with the caveolin-1 from zebrafish, fugu, and pufferfish. In mammals, Tyr14 phosphorylation has emerged recently as a major switch that controls caveolin-1 physiological function in response to extracellular signal molecules and cell stressors such as insulin, IGF-I, EGF, VEGF, PDGF, IL-6, oxidants, hyperosmolarity, and UV irradiation, among others (Fielding, 2006). One interesting feature
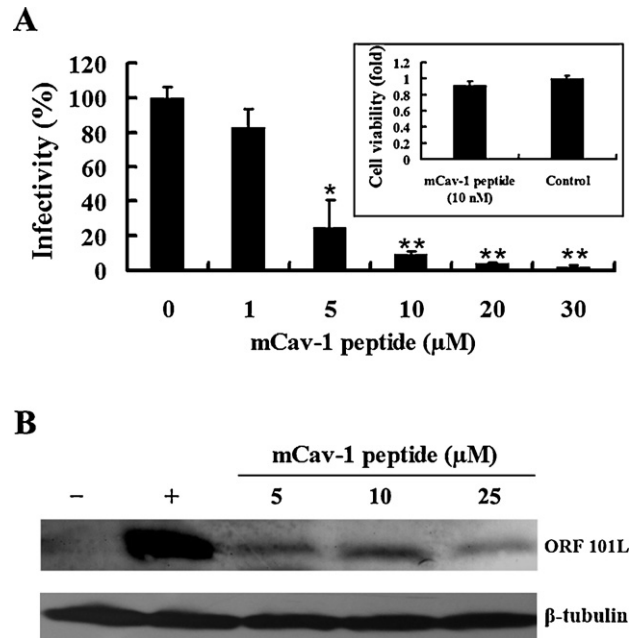
Fig. 6. Effects of mCav-1 scaffolding domain peptide (mSDP) on TFV infection. (A) mSDP effects on ISKNV infection as measured by immunofluorescence staining analysis. Cells were pretreated for 1 h with various concentrations of mSDP, as indicated, or without treatment (0 mM, as a positive control), and incubated with virus for 4 h in presence of mSDP. After 72 h incubation, cells were fixed and processed for immunofluorescence staining with rabbit polyclonal antiserum against ORF100L. Viral infections were quantified as the percentage of positive cells relative to the number of untreated control cells. The viral infectivity of cells untreated with reagents (as positive control) was arbitrarily set as 100%. The data shown are the means and standard deviations of the results from independent experiments. $^*p < 0.05$, $^{**}p < 0.01$. The cytotoxicity of mSDP was evaluated using the (CCK-8). MFF-1 cells were plated in a 96-well plate and incubated at 27 °C for 24 h, at which point the medium was replaced with fresh medium. Cells were then treated with the indicated concentrations of mSDP incubated at 27 °C for an additional 6 h. CCK-8 solution was added to each well, and cells were incubated for 1 h. The absorbance of each well was measured at 450 and 570 nm with an ELISA reader. Absorbance at 570 nm was subtracted from absorbance at 450 nm. Data represents percent cell growth relative to cells treated with control cells for each sample concentration. (B) Effect of mSDP on ISKNV infection determined by Western blot analysis. Cells were treated with mSDP as described above. After 72 h incubation, cells were lysed and processed for Western blot analysis of ORF101L proteins with rabbit polyclonal serum. Endogenous β-tubulin was included as an internal loading control for the Western blot. Lane "+" indicates the control cells untreated with mSDP, and lane "−" indicates the negative controls without ISKNV infection. The concentrations of mSDP are indicated.

that distinguished the caveolin-1 proteins from mandarin fish from those of zebrafish and humans was that caveolin-1 proteins from mandarin fish, fugu, and pufferfish lacked a Tyr-14 residue (Fig. 1B). In addition, we also found that caveolin-1 proteins from mandarin fish, fugu, and pufferfish lacked a reduced Tyr within the first 1–25 amino acids. This indicated that caveolin-1 protein from these three fish did not undergo Tyr14 phosphorylation. Further research is needed to determine whether mCav-1 has mechanisms other than the Tyr14 phosphorylation typical of zebrafish and mammalian caveolin-1 to activate associated-signal events. Our findings may provide a better understanding of the evolution of caveolae-associated molecules and signaling pathways in fish.

In mammalian cells, the major subcellular location of caveolin-1 is at the plasma membrane, which is a defining feature of caveolae. In the present paper, the major subcellular location of mCav-1 was detected in the caveolae (Fig. 2), suggesting that mCav-1 plays its major functional roles there. Caveolae act as organizing centers for signaling molecules in the immune system (Harris et al., 2002), such as the Jak–Stat signal transduction pathway. The important signal molecules of this pathway, the Jak and Stat proteins, have been found in caveolae and directly interact with caveolin-1

protein to inhibit the Jak–Stat signaling pathway (Ju et al., 2000; Park et al., 2002; Shah et al., 2002; Jasmin et al., 2006a). The Jak–Stat transduction pathway plays a critical role in host defenses against viral and bacterial infections and is involved in fish immune system function (Guo et al., 2009). However, the biological roles of caveolin-1 in fish immune responses are still not well understood, including those of the Jak–Stat signal transduction pathway.

In the present study, the effects of caveolin-1 on the Jak–Stat signal transduction pathway were measured in MFF-1 cells by mSDP inhibition. The coupling of molecules to a 16-amino-acid peptide corresponding to the homeodomain of the Drosophila transcription factor *Antennapedia* (AP) is well known to facilitate their uptake into cultured mammalian cells through a non-endocytosis pathway (Perkins et al., 1988; Ou et al., 2003; Jasmin et al., 2006b). Accordingly, coupling of the Cav-1 scaffolding domain to the AP peptide (Cav-1 SDP) was recently shown to facilitate its translocation across the cell membranes and to inhibit signal transduction pathways (Song et al., 2007). Our current results showed that the poly(I:C)-induced Jak–Stat signal transduction pathway strongly induced the expression of *Mx*, *IRF-1*, *SOCS1*, and *SOCS3* genes in MFF-1 cells (Fig. 4), which was consistent with previously reported observations (Guo et al., 2009). However, this enhanced gene expression was significantly impaired by the presence of the mCav-1 scaffolding domain peptide in MFF-1 cells (Fig. 4). These data suggested that one of the functional roles of mCav-1 protein is participation in the Jak–Stat signaling pathway, which is similar to the known role of mammalian caveolin-1. The caveolin-1 scaffolding domain inhibits many of the signal molecules in mammalian cells, such as the endothelial nitric oxide synthase, protein kinase A, thioredoxin reductase 1, transient receptor potential channel-1, etc. (Schlegel et al., 1999; Bucci et al., 2000; Kwiatek et al., 2006; Levin et al., 2007). For this reason, we suggest that caveolae might also act as organizing centers for signaling molecules in the fish immune system.

We found that the expression of mCav-1 protein was clearly increased at 12 h and 24 h in the MFF-1 cells infected with ISKNV (Fig. 5). The mCav-1 protein may therefore play a key role in virus infection. Every virus infection begins with entry of the virus into the host cell. Virus entry is a multi-stage process involving the specific attachment of the virus particle to cell surface receptor(s), followed by internalization of the virus into the cell and subsequent uncoating of the virion to release the capsids or their contents into the cytoplasm (Sánchez-San Martín et al., 2004). Each of these stages represents an important target for combating a virus before it can gain control over the host cell machinery for replication (Rojek et al., 2008). In general, a number of different endocytosis pathway for viruses have been characterized, such as clathrin-mediated endocytosis, caveola-mediated endocytosis, macropinocytosis, etc. (Vidricaire and Tremblay, 2007). Unlike other forms of endocytosis, caveolin-1 is necessary for caveola-dependent endocytosis, as shown by caveolin-1 siRNA experiments or overexpression of caveolin-1 (Nichols, 2003). In our work, ISKNV entry into MFF-1 cells was inhibited when cells were treated with mSDP (Fig. 6). This result indicated that ISKNV entry into MFF-1 cells was associated with caveolae/caveolin-1, and may occur via a caveola-dependent endocytosis pathway. Caveola-dependent endocytosis pathway has been demonstrated for many viruses, such as enterovirus (Stuart et al., 2002), coronavirus 229E (Nomura et al., 2004), and foot-and-mouth disease virus (O'Donnell et al., 2008), etc. Thus, the entry of ISKNV into MFF-1 cells appears to occur via a caveola-dependent endocytosis pathway.

Our research on the function of caveolin-1 aids in understanding the complex signal transduction network that operates in the fish immune system. As well, the cellular entry mechanism of iridoviruses during infection in fish also provides valuable information regarding development of new and effective antiviral targets.

References

Baran, J., Mundy, DI., Vasanji, A., Parat, M.O., 2007. Altered localization of H-Ras in caveolin-1-null cells is palmitoylation-independent. J. Cell Commun. Signal. 1, 195–204.

Beer, C., Andersen, D.S., Rojek, A., Pedersen, L., 2005. Caveola-dependent endocytic entry of amphotropic murine leukemia virus. J. Virol. 79, 10776–10787.

Benferhat, R., Sanchez-Martinez, S., Nieva, J.L., Briand, J.P., Hovanessian, A.G., 2008. The immunogenic CBD1 peptide corresponding to the caveolin-1 binding domain in HIV-1 envelope gp41 has the capacity to penetrate the cell membrane and bind caveolin-1. Mol. Immunol. 45, 1963–1975.

Bucci, M., Gratton, J.P., Rudic, R.D., Acevedo, L., Roviezzo, F., Cirino, G., Sessa, W.C., 2000. In vivo delivery of the caveolin-1 scaffolding domain inhibits nitric oxide synthesis and reduces inflammation. Nat. Med. 6, 1362–1367.

Chelbi-Alix, M.K., Wietzerbin, J., 2007. Interferon, a growing cytokine family: 50 years of interferon research. Biochimie 89, 713–718.

Chen, D., Zangl, A.L., Zhao, Q., Markley, J.L., Zheng, J., Bird, I.M., Magness, R.R., 2001. Ovine caveolin-1: cDNA cloning, E. coli expression, and association with endothelial nitric oxide synthase. Mol. Cell. Endocrinol. 175, 41–56.

Couet, J., Sargiacomo, M., Lisanti, M.P., 1997. Interaction of a receptor tyrosine kinase, EGF-R, with caveolins. Caveolin binding negatively regulates tyrosine and serine/threonine kinase activities. J. Biol. Chem. 272, 30429–30438.

Dong, C., Weng, S., Shi, X., Xu, X., Shi, N., He, J., 2008. Development of a mandarin fish *Siniperca chuatsi* fry cell line suitable for the study of infectious spleen and kidney necrosis virus (ISKNV). Virus Res. 135, 273–281.

Elsasser, T.H., Kahl, S., Li, C.J., Sartin, J.L., Garrett, W.M., Rodrigo, J., 2007. Caveolae nitration of Janus kinase-2 at the 1007Y-1008Y site: coordinating inflammatory response and metabolic hormone readjustment within the somatotropic axis. Endocrinology 148, 3803–3813.

Fielding, C.J., 2006. Lipid Rafts and Caveolae: From Membrane Biophysics to Cell Biology. Wiley, New York, pp. 1–257.

Foster, L.J., De Hoog, C.L., Mann, M., 2003. Unbiased quantitative proteomics of lipid rafts reveals high specificity for signaling factors. Proc. Natl. Acad. Sci. U.S.A. 100, 5813–5818.

Frank, P.G., Pavlides, S., Cheung, M.W., Daumer, K., Lisanti, M.P., 2008. Role of caveolin-1 in the regulation of lipoprotein metabolism. Am. J. Physiol. Cell Physiol. 295, 242–248.

Frank, P.G., Pavlides, S., Lisanti, M.P., 2009. Caveolae and transcytosis in endothelial cells: role in atherosclerosis. Cell Tissue Res. 335, 41–47.

Gao, B., 2005. Cytokines, STATs and liver disease. Cell. Mol. Immunol. 2, 92–100.

Garrean, S., Gao, X.P., Brovkovych, V., Shimizu, J., Zhao, Y.Y., Vogel, S.M., Malik, A.B., 2006. Caveolin-1 regulates NF-kappaB activation and lung inflammatory response to sepsis induced by lipopolysaccharide. J. Immunol. 177, 4853–4860.

Glenney, J.R., Soppet, D., 1992. Sequence and expression of caveolin, a protein component of caveolae plasma membrane domains phosphorylated on tyrosine in Rous sarcoma virus-transformed fibroblasts. Proc. Natl. Acad. Sci. U.S.A. 89, 10517–10521.

Guo, C.J., Zhang, Y.F., Yang, L.S., Yang, X.B., Wu, Y.Y., Liu, D., Chen, W.J., Weng, S.P., Yu, X.Q., He, J.G., 2009. The Jak and Stat family members of the mandarin fish *Siniperca chuatsi*: molecular cloning, tissues distribution and immunobiological activity. Fish Shellfish Immunol. 27, 349–359.

Haller, O., Weber, F., 2009. The interferon response circuit in antiviral host defense. Verh. K. Acad. Geneeskd. Belg. 71, 73–86.

Harris, J., Werling, D., Hope, J.C., Taylor, G., Howard, C.J., 2002. Caveolae and caveolin in immune cells: distribution and functions. Trends Immunol. 23, 158–164.

He, J.G., Zeng, K., Weng, S.P., Chan, S.M., 2000. Systemic disease caused by an iridovirus-like agent in cultured mandarin fish *Siniperca chuatsi* (Basillewsky), in China. J. Fish Dis. 23, 219–222.

He, J.G., Deng, M., Weng, S.P., Li, Z., Zhou, S.Y., Long, Q.X., Wang, X.Z., Chan, S.M., 2001. Complete genome analysis of the mandarin fish infectious spleen and kidney necrosis iridovirus. Virology 291, 126–139.

Horton, M.R., Rädler, J., Gast, A.P., 2006. Phase behavior and the partitioning of caveolin-1 scaffolding domain peptides in model lipid bilayers. J. Colloid Interface Sci. 304, 67–76.

Ikonen, E., Parton, R.G., 2000. Caveolins and cellular cholesterol balance. Traffic 1, 212–217.

Imada, K., Leonard, W.J., 2000. The Jak-Stat pathway. Mol. Immunol. 37, 1–11.

Jasmin, J.F., Mercier, I., Sotgia, F., Lisanti, M.P., 2006a. SOCS proteins and caveolin-1 as negative regulators of endocrine signaling. Trends Endocrinol. Metab. 17, 150–158.

Jasmin, J.F., Mercier, I., Dupuis, J., Tanowitz, H.B., Lisanti, M.P., 2006b. Short-term administration of a cell-permeable caveolin-1 peptide prevents the development of monocrotaline-induced pulmonary hypertension and right ventricular hypertrophy. Circulation 114, 912–920.

Ju, H., Zou, R., Venema, V.J., Venema, R.C., 1997. Direct interaction of endothelial nitric-oxide synthase and caveolin-1 inhibits synthase activity. J. Biol. Chem. 272, 18522–18525.

Ju, H., Venema, V.J., Liang, H., Harris, M.B., Zou, R., Venema, R.C., 2000. Bradykinin activates the Janus-activated kinase/signal transducers and activators of transcription (JAK/STAT) pathway in vascular endothelial cells: localization of JAK/STAT signalling proteins in plasmalemmal caveolae. Biochem. J. 351, 257–264.

Kim, H., Ahn, M., Lee, J., Moon, C., Matsumoto, Y., Koh, C.S., Shin, T., 2006. Increased phosphorylation of caveolin-1 in the spinal cord of Lewis rats with experimental autoimmune encephalomyelitis. Neurosci. Lett. 402, 76–80.

Kizhatil, K., Albritton, L.M., 1997. Requirements for different components of the host cell cytoskeleton distinguish ecotropic murine leukemia virus entry via endocytosis from entry via surface fusion. J. Virol. 71, 7145–7156.

Kurzchalia, T.V., Dupree, P., Parton, R.G., Kellner, R., Virta, H., Lehnert, M., Simons, K., 1992. VIP21, a 21-kD membrane protein is an integral component of trans-Golgi-network-derived transport vesicles. J. Cell Biol. 118, 1003–1014.

Kwiatek, A.M., Minshall, R.D., Cool, D.R., Skidgel, R.A., Malik, A.B., Tiruppathi, C., 2006. Caveolin-1 regulates store-operated Ca^{2+} influx by binding of its scaffolding domain to transient receptor potential channel-1 in endothelial cells. Mol. Pharmacol. 70, 1174–1183.

Lad, S.P., Fukuda, E.Y., Li, J., de la Maza, L.M., Li, E., 2005. Up-regulation of the JAK/STAT1 signal pathway during Chlamydia trachomatis infection. J. Immunol. 174, 7186–7193.

Lavialle, F., Rainteau, D., Massey-Harroche, D., Metz, F., 2000. Establishment of plasma membrane polarity in mammary epithelial cells correlates with changes in prolactin trafficking and in annexin VI recruitment to membranes. Biochim. Biophys. Acta 1464, 83–94.

Lee, C.J., Lin, H.R., Liao, C.L., Lin, Y.L., 2008. Cholesterol effectively blocks entry of flavivirus. J. Virol. 82, 6470–6480.

Lee, S.H., Kim, J.S., Jun, H.K., Lee, H.R., Lee, D., Choi, B.K., 2009. The major outer membrane protein of a periodontopathogen induces IFN-beta and IFN-stimulated genes in monocytes via lipid raft and TANK-binding kinase 1/IFN regulatory factor-3. J. Immunol. 182, 5823–5835.

Levin, A.M., Murase, K., Jackson, P.J., Flinspach, M.L., Poulos, T.L., Weiss, G.A., 2007. Double barrel shotgun scanning of the caveolin-1 scaffolding domain. ACS Chem. Biol. 2, 493–500.

Levy, D.E., Darnell Jr., J.E., 2002. Stats: transcriptional control and biological impact. Nat. Rev. Mol. Cell Biol. 3, 651–662.

Liu, J., Cui, Y., Liu, J., 1998. Food consumption and growth of two piscivorous fishes, the mandarin fish and the Chinese snakehead. J. Fish Biol. 53, 1071–1083.

Liu, J., Cui, Y., Liu, J., 2000. Resting metabolism and heat increment of feeding in the mandarin fish (Siniperca chuatsi) and the Chinese snakehead (Channa argus). Comp. Biochem. Physiol. 127, 131–138.

Muller, P.Y., Janovjak, H., Miserez, A.R., Dobbie, Z., 2002. Processing of gene expression data generated by quantitative real-time RT-PCR. Biotechniques 32, 1372–1374, 1376, 1378–1379.

Nichols, B., 2003. Caveosomes and endocytosis of lipid rafts. J. Cell Sci. 116, 4707–4714.

Nomura, R., Kiyota, A., Suzaki, E., Kataoka, K., Ohe, Y., Miyamoto, K., Senda, T., Fujimoto, T., 2004. Human coronavirus 229E binds to CD13 in rafts and enters the cell through caveolae. J. Virol. 78, 8701–8718.

O'Donnell, V., Larocco, M., Baxt, B., 2008. Heparan sulfate-binding foot-and-mouth disease virus enters cells via caveola-mediated endocytosis. J. Virol. 82, 9075–9085.

Ou, J., Geiger, T., Ou, Z., Ackerman, A.W., Oldham, K.T., Pritchard Jr., K.A., 2003. AP-4F, antennapedia peptide linked to an amphipathic alpha helical peptide, increases the efficiency of Lipofectamine-mediated gene transfection in endothelial cells. Biochem. Biophys. Res. Commun. 305, 605–610.

Palade, G.E., 1953. An electron microscope study of the mitochondrial structure. J. Histochem. Cytochem. 1, 188–211.

Park, D.S., Lee, H., Frank, P.G., Razani, B., Nguyen, A.V., Parlow, A.F., Russell, R.G., Hulit, J., Pestell, R.G., Lisanti, M.P., 2002. Caveolin-1-deficient mice show accelerated mammary gland development during pregnancy, premature lactation, and hyperactivation of the Jak-2/Stat5a signaling cascade. Mol. Biol. Cell 13, 3416–3430.

Parkin, E.T., Turner, A.J., Hooper, N.M., 1996. Isolation and characterization of two distinct low-density, Triton-insoluble, complexes from porcine lung membranes. Biochem. J. 319, 887–896.

Perkins, K.K., Dailey, G.M., Tjian, R., 1988. In vitro analysis of the Antennapedia P2 promoter: identification of a new Drosophila transcription factor. Genes Dev. 2, 1615–1626.

Rath, G., Dessy, C., Feron, O., 2009. Caveolae, caveolin and control of vascular tone: nitric oxide (NO) and endothelium derived hyperpolarizing factor (EDHF) regulation. J. Physiol. Pharmacol. 4, 105–109.

Razani, B., Park, D.S., Miyanaga, Y., Ghatpande, A., Cohen, J., Wang, X.B., Scherer, P.E., Evans, T., Lisanti, M.P., 2002. Molecular cloning and developmental expression of the caveolin gene family in the amphibian Xenopus laevis. Biochemistry 41, 7914–7924.

Rojek, J.M., Perez, M., Kunz, S., 2008. Cellular entry of lymphocytic choriomeningitis virus. J. Virol. 82, 1505–1517.

Rothberg, K.G., Heuser, J.E., Donzell, W.C., Ying, Y.S., Glenney, J.R., Anderson, R.G., 1992. Caveolin, a protein component of caveolae membrane coats. Cell 68, 673–682.

Sánchez-San Martín, C., López, T., Arias, C.F., López, S., 2004. Characterization of rotavirus cell entry. J. Virol. 78, 2310–2318.

Sarasin-Filipowicz, M., Wang, X., Yan, M., Duong, F.H., Poli, V., Hilton, D.J., Zhang, D.E., Heim, M.H., 2009. Alpha interferon induces long-lasting refractoriness of JAK–STAT signaling in the mouse liver through induction of USP18/UBP43. Mol. Cell. Biol. 29, 4841–4851.

Sargiacomo, M., Sudol, M., Tang, Z., Lisanti, M.P., 1993. Signal transducing molecules and glycosyl-phosphatidylinositol-linked proteins form a caveolin-rich insoluble complex in MDCK cells. J. Cell Biol. 122, 789–807.

Scherer, P.E., Okamoto, T., Chun, M., Nishimoto, I., Lodish, H.F., Lisanti, M.P., 1996. Identification, sequence and expression of caveolin-2 defines a caveolin gene family. Proc. Natl. Acad. Sci. U.S.A. 93, 131–135.

Schlegel, A., Schwab, R.B., Scherer, P.E., Lisanti, M.P., 1999. A role for the caveolin scaffolding domain in mediating the membrane attachment of caveolin-1. The caveolin scaffolding domain is both necessary and sufficient for membrane binding in vitro. J. Biol. Chem. 274, 22660–22667.

Schutzer, W.E., Reed, J.F., Mader, S.L., 2005. Decline in caveolin-1 expression and scaffolding of G protein receptor kinase-2 with age in Fischer 344 aortic vascular smooth muscle. Am. J. Physiol. Heart Circ. Physiol. 288, 2457–2464.

Shah, M., Patel, K., Fried, V.A., Sehgal, P.B., 2002. Interactions of STAT3 with caveolin-1 and heat shock protein 90 in plasma membrane raft and cytosolic complexes. Preservation of cytokine signaling during fever. J. Biol. Chem. 277, 45662–45669.

Smart, E.J., Ying, Y.S., Mineo, C., Anderson, R.G., 1995. A detergent-free method for purifying caveolae membrane from tissue culture cells. Proc. Natl. Acad. Sci. U.S.A. 92, 10104–10108.

Song, K.S., Li, S., Okamoto, T., Quilliam, L.A., Sargiacomo, M., Lisanti, M.P., 1996. Co-purification and direct interaction of Ras with caveolin, an integral membrane protein of caveolae microdomains. Detergent-free purification of caveolae microdomains. J. Biol. Chem. 271, 9690–9697.

Song, L., Ge, S., Pachter, J.S., 2007. Caveolin-1 regulates expression of junction-associated proteins in brain microvascular endothelial cells. Blood 109, 1515–1523.

Stuart, A.D., Eustace, H.E., McKee, T.A., Brown, T.D., 2002. A novel cell entry pathway for a DAF-using human enterovirus is dependent on lipid rafts. J. Virol. 76, 9307–9322.

Sun, B.J., Nie, P., 2004. Molecular cloning of the viperin gene and its promoter region from the mandarin fish Siniperca chuatsi. Vet. Immunol. Immunopathol. 101, 161–170.

Tang, Z.L., Scherer, P., Lisanti, M.P., 1994. The primary sequence of murine caveolin reveals a conserved consensus site for phosphorylation by protein kinase C. Gene 147, 299–300.

Tang, Z., Scherer, P.E., Okamoto, T., Song, K., Chu, C., Kohtz, D.S., Nishimoto, I., Lodish, H.F., Lisanti, M.P., 1996. Molecular cloning of caveolin-3, a novel member of the caveolin gene family expressed predominantly in muscle. J. Biol. Chem. 71, 2255–2261.

Thomas, C.M., Smart, E.J., 2008. Caveolae structure and function. J. Cell. Mol. Med. 12, 796–809.

Thompson, J.D., Gibson, T.J., Plewniak, F., Jeanmougin, F., Higgins, D.G., 1997. The CLUSTAL_X windows interface: flexible strategies for multiple sequence alignment aided by quality analysis tools. Nucleic Acids Res. 25, 4876–4882.

Vidricaire, G., Tremblay, M.J., 2007. A clathrin, caveolae, and dynamin-independent endocytic pathway requiring free membrane cholesterol drives HIV-1 internalization and infection in polarized trophoblastic cells. J. Mol. Biol. 368, 1267–1283.

Way, M., Parton, R.G., 1996. M-caveolin, a muscle-specific caveolin-related protein. FEBS Lett. 378, 108–112.

Williams, T.M., Lisanti, M.P., 2004. The caveolin proteins. Genome Biol. 5, 214–217.

Zhang, Y.A., Nie, P., Wang, Y.P., Zhu, Z.Y., 2003. cDNA sequence encoding immunoglobulin M heavy chain of the mandarin fish Siniperca chuatsi. Fish Shellfish Immunol. 14, 477–480.